Timing Synchronization in High Mobility OFDM Systems

Yasamin Mostofi
Department of Electrical Engineering
Stanford University
Stanford, CA 94305, USA
Email: yasi@wireless.stanford.edu

Donald C. Cox
Department of Electrical Engineering
Stanford University
Stanford, CA 94305, USA
Email: dcox@spark.stanford.edu

***Abstract*— OFDM systems are sensitive to timing synchronization errors. Utilizing pilot-aided channel estimators in OFDM systems can further increase this sensitivity. This is shown in [2] where authors have analyzed the effect of such errors on a pilot-aided channel estimator in a fixed wireless environment. They proposed an algorithm that exploits this sensitivity to improve timing synchronization without additional training overhead. The effect of these errors and design of suitable synchronization algorithms for *high mobility* applications, however, have not been studied before. In this paper we extend the analysis in [2] to high mobility environments. Timing synchronization becomes more challenging for mobile applications since power-delay profile of the channel may change rapidly due to the sporadic birth and death of the channel paths. We find analytical expressions for channel estimation error in the presence of timing synchronization errors and mobility. We show that the sensitivity of the channel estimator can still be exploited to improve timing synchronization in high mobility environments. Then we extend the algorithm proposed in [2] to high mobility applications. Finally simulation results show the performance of the algorithm in high delay and Doppler spread environments.**

I. INTRODUCTION

Orthogonal Frequency Division Multiplexing (OFDM) systems divide the given bandwidth into narrow sub-channels. By transmitting low data rates in parallel on these sub-channels, OFDM systems can handle high delay spread environments [1]. The performance of OFDM systems, however, is sensitive to the performance of the timing synchronizer and channel estimator (in this paper, timing synchronization refers to the correct detection of the start of an OFDM symbol). Furthermore, high mobility can introduce time-variations in one OFDM symbol, which ruins the performance. Each of these issues has been mainly explored separately. Research in timing synchronization has mainly focused on fixed wireless applications and can be primarily categorized into two groups: Training-based and correlation-based. The first group is based on transmitting two identical symbols [7]. Muller [5] has provided a good survey and comparison of such algorithms. The performance of these methods is good but there is a waste of bandwidth in transmitting the training information. The second category is based on using the redundancy of the cyclic prefix [8]. Then the start of the symbol is where the correlation of the start and end data points is maximized. In the absence of delay spread, this would work fine. However, in the presence of delay spread, the cyclic prefix would be affected by the previous OFDM symbol resulting in performance degradation. There are other methods that use cyclic prefix for coarse synchronization followed by a fine tuning [9]. However, Yang in [9] makes the assumption that the first channel tap is the strongest, which may not be the case in environments with no line of sight path.

To estimate the channel in high delay spread OFDM applications, it is necessary to transmit pilot tones. If maximum channel delay spread spans ν sampling periods, Negi et al. [6] has shown that only $L = \nu+1$ equally-spaced pilots are needed for channel estimation. To get an estimate of the channel at all the sub-carriers, an IFFT of length L, zero padding and an FFT of length N should be performed, where N represents the number of sub-carriers. There are other less optimum ways of interpolating the channel in between pilot sub-carriers. As delay spread increases, the performance of these sub-optimum methods degrades drastically. Therefore they are not the focus of this paper as we are interested in high delay spread environments. Most of the work in timing synchronization and channel estimation has looked at these issues separately. To understand the effect of timing synchronization errors on channel estimation, authors in [2] took at overall look at both issues. They showed the super-sensitivity of the pilot-aided channel estimator to timing synchronization errors. Based on their analysis, they proposed a robust timing synchronization algorithm that utilizes this sensitivity to correct for timing synchronization errors without additional training overhead.

Timing synchronization becomes more challenging in high mobility environments. For such applications, applying training-based algorithms for timing synchronization can increase the training overhead considerably. Furthermore, utilizing correlation-based methods would result in performance degradation due to high delay spread. Therefore the method proposed by Mostofi et al. [2] can be a good candidate for such applications. In [2], the analysis was performed for fixed wireless applications and the effect of mobility was not studied. It is the goal of this paper to take mobility into account. We show that the sensitivity of the channel estimator can still be exploited to improve timing synchronization in high mobility environments. Based on the analysis, we extend the algorithm proposed in [2] to high mobility applications.

We show both analytically and through simulation results that the algorithm works robustly in high delay and Doppler spread environments.

II. SYSTEM MODEL

Consider an OFDM system in which the given bandwidth is divided into N sub-channels and the guard interval spans G sampling periods. We assume that the length of the channel is always less than or equal to G in this paper. X_i represents the transmitted data point in the i^{th} sub-channel and is related to time-domain sequence, x, as $X_i = \sum_{k=0}^{N-1} x_k e^{-\frac{j2\pi ki}{N}}$. Sequences y and its FFT, Y, are the received data points in time and frequency domain respectively and w_i is AWGN. Let T be the time duration of one OFDM symbol after adding the guard interval. Then, $h_q^{(k)}$ represents the q^{th} channel tap at time $t = k \times T_s$ where $T_s = \frac{T}{N+G}$. A constant channel is assumed over the time interval $k \times T_s \leq t < (k+1) \times T_s$ with $t = 0$ indicating the start of the data part of the symbol.

A. Ideal case: no mobility and perfect synchronization

In this case, we drop the superscript k as $h_q^{(k)}$ will not be a function of k. If H denotes the FFT of the channel, h, then at the i^{th} sub-channel, we will have $Y_i = H_i X_i + W_i$,where W is the FFT of w. Let $H_{eq}(i) = \sum_k h_{eq}(k) e^{-\frac{j2\pi ik}{N}}$ represent the relationship between X_i and Y_i. Then in this case we will have $H_{eq}(i) = H_i$. Let ν be the maximum predicted normalized length of the channel delay spread. Therefore, only $L = \nu + 1$ equally-spaced pilot tones, $X_{pl}(l_i)$ for $0 \leq i \leq L-1$, are needed to estimate channel frequency-variations where $l_i = \frac{i \times N}{L}$. Then,

$$\hat{H}_{eq}(l_i) = \frac{Y_{l_i}}{X_{pl}(l_i)} = H_{eq}(l_i) + \frac{W_{l_i}}{X_{pl}(l_i)} \quad 0 \leq i \leq L-1 \quad (1)$$

Through an IFFT of length L, the estimate of the channel in time-domain would be $\hat{h}_{eq}(k) = \frac{1}{L}\sum_{i=0}^{L-1} \hat{H}_{eq}(l_i) e^{\frac{j2\pi ik}{L}}$ for $0 \leq k \leq L-1$. Then through an FFT of length N, the estimate of the channel at all the sub-carriers is $\hat{H}_{eq}(i) = \sum_{k=0}^{L-1} \hat{h}_{eq}(k) e^{-\frac{j2\pi ik}{N}}$ for $0 \leq i \leq N-1$.

B. Case of mobility with perfect synchronization

In this case, the time-domain received signal, $y_{mob,k}$ is:

$$y_{mob,k} = \underbrace{\sum_q h_q^{(k)} x_{((k-q))_N}}_{\vartheta_{mob,k}} + w_k \quad 0 \leq k \leq N-1 \quad (2)$$

The subscript mob distinguishes the mobile case from the previous case and $((\quad))_N$ refers to a cyclic shift in the base of N. By taking an FFT of $y_{mob,k}$, the frequency-domain received signal will be:

$$Y_{mob,i} = H_{i,0} X_i + \underbrace{\sum_{z=1}^{N-1} H_{i,z} X_{((i-z))_N}}_{ICI_{mob}(i)} + W_i \quad 0 \leq i \leq N-1 \quad (3)$$

The second term on the right hand side of Eq. 3 represents the Inter-Carrier-Interference (ICI) introduced by mobility. It can be easily shown that $H_{i,z}$ is as follows, $H_{i,z} = \frac{1}{N}\sum_{g=0}^{C}\sum_{g'=0}^{N-1} h_g^{(g')} e^{-\frac{j2\pi}{N}(z \times (g'-g) + g \times i)}$ where $C \leq \nu$ represents normalized length of the channel delay spread. In this case, $H_{mob,eq}(i) = H_{i,0}$. Following the same procedure of the previous sub-section, an estimate of $H_{mob,eq}(i)$ can be acquired using the pilots. In this case, L pilots may not be enough to estimate the channel. Different methods can be used to mitigate the effect of mobility. This paper will not focus on mobility mitigation since the main objective of the paper is to achieve robust timing synchronization in the presence of mobility. For more on mobility mitigation, refer to [3].

C. Case of timing synchronization errors and mobility

Consider a case that a timing error of m sampling periods has occurred. $m > 0$ and $m < 0$ denote timing errors of m to the right and left side of the start of the OFDM symbol respectively.

1) Case of $m > 0$ in the presence of mobility: In this case, an error of m sampling periods to the right side has occurred. Then, the terms $y_{mob,0}, y_{mob,1}, \cdots, y_{mob,m-1}$ are missed and instead m data points of the next OFDM symbol are erroneously selected. The received signal can thus be written as follows:

$$y_{mob,k}^r = \vartheta_{mob,((k+m))_N} \times \gamma_k^r + s_k + w_k^r \quad 0 \leq k \leq N-1 \quad (4)$$

where the superscript r denotes the case of $m > 0$. w_k^r is AWGN, $\gamma_k^r = \begin{cases} 1 & 0 \leq k \leq N-m-1 \\ 0 & N-m \leq k \leq N-1 \end{cases}$ and $s_k = \begin{cases} 0 & 0 \leq k \leq N-m-1 \\ y_{mob,pf}^{next}(k-N+m) & else \end{cases}$. $y_{mob,pf}^{next}(k)$ represents the k^{th} sample of the output cyclic prefix of the next OFDM symbol in the presence of mobility. It can be easily shown that the FFT of $y_{mob,k}^r$ will be as follows:

$$Y_{mob,i}^r = \overbrace{\underbrace{e^{\frac{j2\pi mi}{N}} F_i^r}_{H_{mob,eq}^r(i)} X_i}^{signal} + \overbrace{W_{mob}^r(i)}^{noise} + \overbrace{\underbrace{\frac{\Gamma_0^r}{N} e^{\frac{j2\pi mi}{N}} ICI_{mob}(i) + ICI_{mob}^r(i)}_{correlated \quad terms} + ISI_{mob}^r(i)}^{interference} \quad (5)$$

where $F_i^r = \sum_{z=0}^{N-1} e^{-j\frac{2\pi mz}{N}} \frac{\Gamma_z^r}{N} H_{((i-z))_N, N-z}$, Γ^r is the FFT of γ^r and W_{mob}^r is AWGN. ICI_{mob} is as defined in Eq. 3. ICI_{mob}^r and ISI_{mob}^r are the ICI and ISI (Inter-OFDM Symbol-Interference) terms introduced by timing synchronization errors. Due to the effect of mobility, their expressions are different from the case of fixed wireless. Using the expressions of the interference terms and after a long derivation, an expression can be derived for $SIR_{mob}^r(m)$, the average Signal to Interference Ratio for the case of $m > 0$ in the presence of mobility [4].

2) Case of $m < 0$ in the presence of mobility: In this case, due to the presence of the cyclic prefix, the number of data points that are missed can be less than $-m$ [2]. If the length of the channel delay spread spans $C \leq \nu$ sampling periods, only $d = max(C - (G+m), 0)$ data points are corrupted due to the interference from the previous symbol. Therefore the time-domain received signal in this case will be,

$$y^l_{mob,k} = \vartheta_{mob,((k+m))_N} \times \gamma^l_k + p_k + w^l_k \quad 0 \leq k \leq N-1 \quad (6)$$

where the superscript l denotes the case of $m < 0$. w^l_k is AWGN, $\gamma^l_k = \begin{cases} 0 & 0 \leq k \leq d-1 \\ 1 & d \leq k \leq N-1 \end{cases}$ and $p_k = \begin{cases} 0 & d \leq k \leq N-1 \\ y_{mob,pf}(G+m+k) & else \end{cases}$. $y_{mob,pf}(k)$ represents the k^{th} sample of the output cyclic prefix of the current OFDM symbol in the presence of mobility. It can be easily shown that the FFT of y^l_{mob} will be as follows:

$$\begin{aligned} Y^l_{mob,i} &= e^{\frac{j2\pi mi}{N}} F^l_i X_i + \frac{\Gamma^l_0}{N} e^{\frac{j2\pi mi}{N}} ICI_{mob}(i) \\ &+ ICI^l_{mob}(i) + ISI^l_{mob}(i) + W^l_{mob}(i) \quad (7) \end{aligned}$$

where F^l_i is defined similar to the case of $m > 0$, Γ^l is the FFT of γ^l, W^l_{mob} is AWGN and $H^l_{mob,eq}(i) = e^{\frac{j2\pi mi}{N}} F^l_i$. Similarly, an expression can be derived for $SIR^l_{mob}(m)$ [4]. Timing errors for the case of $m < 0$ can result in lower interference than the case of $m > 0$ (or no interference) due to the presence of cyclic prefix.

III. Effect of Timing Errors on Channel Estimation in the Presence of Mobility

In this section we explore the effect of timing errors on the performance of a pilot-aided channel estimator. Consider the case of $m \geq 0$. Through an IFFT of $H^r_{mob,eq}$, the time-domain equivalent channel will be $h^r_{mob,eq}(k) = f^r_{((k+m))_N}$, with f^r representing the IFFT of F^r. Timing synchronization error introduces a rotation of m sampling periods in the base of N in the equivalent channel. It can be easily proved that f^r has the same length as the channel delay spread. Therefore, this rotation will result in the expansion of the channel beyond its maximum predicted length. Fig. 1b shows the equivalent channel for an f^r of length $L-1$ shown in Fig. 1a. As can be seen, a rotation has occurred and resulted in the expansion of the equivalent channel beyond the maximum predicted length of ν. Even one error to the right side will result in an equivalent channel of length $N-1$. This will degrade the performance of the channel estimator, as it assumes an equivalent channel that spans ν sampling periods at maximum. To see the effect of timing errors on channel estimation analytically, consider the case that L equally-spaced pilot tones are inserted among the sub-carriers. It can be easily shown that the time-domain channel estimate can be expressed as follows:

$$\hat{h}^r_{mob,eq}(k) = f^r_{((k+m))_L} + \underbrace{u^r_k}_{Interference} + \underbrace{v^r_k}_{AWGN} \quad (8)$$

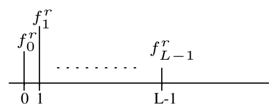

Fig. 1a Original channel (length $L-1$)

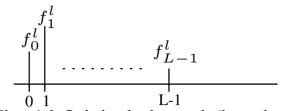

Fig. 1d Original channel (length $L-1$)

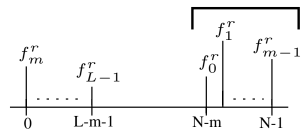

Fig. 1b Equivalent channel ($m \geq 1$)

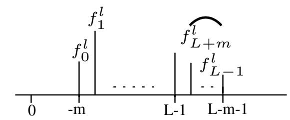

Fig. 1e Equivalent channel ($m \leq -1$)

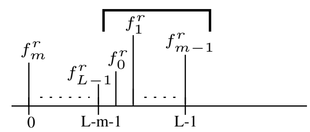

Fig. 1c Estimated channel ($m \geq 1$)

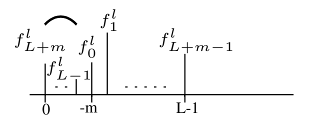

Fig. 1f Estimated channel ($m \leq -1$)

As can be seen from Eq. 8, there are three factors contributing to channel estimation error: effect of rotation, interference and noise. The first factor is caused since the equivalent channel has a rotation in the base of N while the estimated equivalent channel has a rotation in the base of L. Since L is chosen based on the maximum predicted length of the original channel, ν, it is typically considerably smaller than N. Therefore, channel estimation error can be considerable, solely due to the first factor. Fig. 1c shows the estimated equivalent channel for the equivalent channel of Fig. 1b (effect of interference and noise is not shown on the figure). Comparing Fig. 1b and 1c, a mismatch can be observed in the location of the first m taps of the original channel of Fig. 1a (original channel refers to f^r in the absence of rotation). Since these taps are typically strong, this can result in a considerable performance degradation of the channel estimator. To analytically assess the contribution of each of the aforementioned factors, next we derive an expression for channel estimation error:

$$\Delta H^r_{mob,eq}(i) = \sum_{k=0}^{m-1} \beta_{i,k} f^r_k + U^r_i + V^r_i \quad 0 \leq i \leq N-1 \quad (9)$$

where $\Delta H^r_{mob,eq}$ represents the frequency-domain channel estimation error with $U^r_i = \sum_{z=0}^{L-1} \alpha_{i,z} \frac{\frac{\Gamma^r_0}{N} e^{\frac{j2\pi m l_z}{N}} ICI_{mob}(l_z) + ICI^r_{mob}(l_z) + ISI^r_{mob}(l_z)}{X_{pl}(l_z)}$ and $V^r_i = \sum_{z=0}^{L-1} \alpha_{i,z} \frac{W^r_{mob}(l_z)}{X_{pl}(l_z)}$ representing the FFTs of u^r and v^r. $l_z = \frac{N}{L} z$, $\alpha_{i,z} = \frac{1}{L} \sum_{o=0}^{L-1} e^{j2\pi o(\frac{z}{L} - \frac{i}{N})}$ and $\beta_{i,k} = e^{\frac{-j2\pi i(k-m)}{N}} \times (1 - e^{-\frac{j2\pi iL}{N}})$. After a long derivation, normalized channel estimation error at i^{th} sub-carrier, $E^r(m,i)$, can be tightly approximated as:

$$\begin{aligned} E^r(m,i) &= \frac{\overline{|\Delta H^r_{mob,eq}(i)|^2}}{\overline{|H^r_{mob,eq}(i)|^2}} = \underbrace{4P^r_{\%}(m) sin^2(\frac{\pi i L}{N})}_{factor\#1: rotation \quad effect} \\ &+ \frac{1}{SIR^r_{mob}(m)} + \frac{1}{SNR^r_{mob}(m)} \quad (10) \end{aligned}$$

where $SNR^r_{mob}(m) = \frac{\sigma^2_X \sigma^2_H}{N^2 \sigma^2_W} \sum_{z=m}^{N-1} \sum_{z'=m}^{N-1} R_n((z-z')T_s)$ and SIR^r_{mob} is as defined in Section II. $R_n(zT_s)$ is the normalized auto-correlation function of channel taps. In deriving Eq. 10, the same normalized auto-correlation function is assumed for all the taps. This assumption is not required for the analysis and design of a robust timing synchronizer in the rest of the paper. σ_X^2 and σ_W^2 are average powers of X and W respectively. $P_{\%}^r(m)$ represents the ratio of the power of the mismatched taps to the total power of the channel and σ_H^2 represents total channel power. Compared with the channel estimation error derived in [2], rotation has the same contribution as it had in the fixed wireless case. The second and third terms on the right hand side of Eq. 10, however, have slightly higher values compared to their corresponding terms in the fixed wireless case. Still, the effect of rotation is the major contributor to channel estimation error as the first term gets considerably high values. *factor#1* does not affect pilot sub-channels. However, it results in a considerable increase of error for other sub-carriers particularly those at $i = o_{odd} \times ceil(\frac{N}{2L})$, where o_{odd} represents odd integers. To see the effect of $factor\#1$, Fig. 2 shows $E^r(m,i)$ for the sub-carriers in the middle of every two consecutive pilots and for different levels of mobility. $f_{d,norm}$ refers to the percentage of the maximum Doppler spread divided by sub-carrier spacing and each channel tap has Jakes power-spectrum. As can be seen, mobility does not have a distinguishable impact on channel estimation error for $f_{d,norm}$ as high as 20% since the effect of rotation is very high. To see the contribution of the rotation factor, the solid line shows the effect of the first term solely. As can be seen, $factor\#1$ is almost 100% contributor to channel estimation error at low m. As m approaches the length of the guard interval, ICI and ISI introduced by timing synchronization error increase. Still, $factor\#1$ contributes to more than 80% of channel estimation error at $m = G$. To examine a case where Doppler spread has a distinguishable impact on channel estimation error, we increase $f_{d,norm}$ to 50%. It should be noted that even in case of a perfect timing synchronization, such a high Doppler level would ruin the performance of an OFDM system drastically and therefore is not a realistic scenario. Even for such a high Doppler level, *factor#1* contributes to more that 70% of channel estimation error. The timing synchronization method proposed in [2] was effective as long as *factor#1* is the major contributor to channel estimation error. As was shown, mobility does not have a considerable impact on channel estimation in the presence of timing errors. Therefore, extending the method proposed in [2] should provide robust timing synchronization for high mobility applications.

Similar expressions can be derived for the case of $m < 0$. We will have $h^l_{mob,eq}(k) = f^l_{((k+m))_N}$ and $\hat{h}^l_{mob,eq}(k) = f^l_{((k+m))_L} + u^l_k + v^l_k$. Fig. 1e and 1f show the equivalent and estimated equivalent channel for f^l of Fig. 1d respectively. On the contrary to the case of $m > 0$ where even one error to the right resulted in an equivalent channel of length $N-1$ (see Fig. 1b), the equivalent channel length for $m < 0$ varies depending on the length of the channel. For instance, for a channel of length $C \leq \nu$, the equivalent channel length will be $C - m$ for $m \leq -1$. Therefore for $C - \nu \leq m \leq -1$, the equivalent length would still be less than or equal to ν, which poses no problem for the channel estimator. Furthermore, the mismatch is in the location of the last m taps of the original channel which are not typically that strong. Depending on the length of the channel, these taps can be solely occupied by noise/interference. Therefore, we see again that errors to the left side may not cause any performance degradation depending on the length of the channel delay spread, guard interval and number of pilots.

Fig. 2 Effect of mobility on channel estimation error

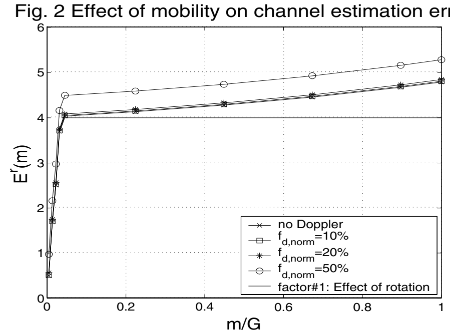

IV. Timing synchronization error correction

We showed that pilot-aided channel estimator is super-sensitive to timing synchronization errors due to the effect of rotation. We also showed that in a mobile environment, effect of rotation is still the dominant cause of channel estimation performance degradation. Therefore, this sensitivity can be exploited to design a synchronization algorithm that works robustly in high mobility environments. After a coarse timing synchronizer has detected a start point for the symbol (a correlation-based synchronizer can be used for this), $\hat{H}_{mob,eq}$ can be obtained using pilots. In the presence of timing errors, this channel estimate may be far from $H_{mob,eq}$. Call $\hat{X}_i = \frac{Y_{mob,i}}{\hat{H}_{mob,eq}(i)}$, the estimated input at i^{th} sub-channel. Let $\tilde{X}_i = Dec(\hat{X}_i)$ represent the estimated input after passing through the decision device. Define a decision-directed measure function as $M = \sum_{i=0}^{N-1} |\hat{X}_i - \tilde{X}_i|^2$. In the presence of channel rotation, M can become very large. Therefore, synchronization error correction can be obtained iteratively by minimizing M. Note that we detect timing errors solely due to the large impact of *factor#1* on the performance. Therefore, as long as *factor#1* is the major cause of performance loss, which is the case with high probability, we can detect timing errors. Due to the large contribution of rotation, it is possible to perform all the updates necessary to find the best timing correction solely in the frequency domain. Consider correcting errors to the right. As can be seen from Fig. 1c, the position of the last m taps of the estimated channel is different from that of the equivalent channel, where m is unknown. Therefore through an iterative process, we update the estimated channel, correcting for one mismatched tap at a time. Then the update necessary for correcting errors to the right at the k^{th} iteration and i^{th} sub-channel will be as follows:

$$\hat{H}^{(k+1),r}_{mob,eq}(i) = \hat{H}^{(k),r}_{mob,eq}(i) + c_1 \times \hat{h}^{r}_{mob,eq}(L-k) \times e^{j2\pi ik/N} \quad (11)$$

Similarly, we will have $\hat{H}^{(k+1),l}_{mob,eq}(i) = \hat{H}^{(k),l}_{mob,eq}(i) - c_1 \times \hat{h}^{l}_{mob,eq}(k-1) \times e^{-j2\pi(k-1)i/N}$ for detecting errors to the left, where $c_1 = 1 - e^{-\frac{j2\pi L}{N}}$ and $\hat{H}^{(1),r}_{mob,eq}(i) = \hat{H}^{(1),l}_{mob,eq}(i) = \hat{H}_{mob,eq}(i)$. In each iteration, the measure function, $M^{(k)}$, will be evaluated. Finally the iteration with smallest M is chosen and the correction necessary would be applied to the start of the symbol in time-domain.

V. Simulation Results

We simulate an OFDM system in a time-variant environment with high delay spread as is the case for an SFN (Single Frequency Network) channel. We choose the following system parameters based on Sirius Radio (a DAB service provider) second generation system specification proposal. Input modulation is 8PSK. Bit rate is 7.3Mbps, N=892 and L=223. Power-delay profile of the simulated channel is shown in Fig. 3. It has two main clusters each with 9 taps to represent an SFN channel. Channel delay spread is $36.5\mu s$ spanning 64% of the guard interval. Each channel tap is generated as a random process with Rayleigh distributed amplitude and uniformly distributed phase using Jakes model. The auto-correlation of each tap is zero-order Bessel function. It was shown in [2] that the proposed algorithm can reduce the error profile very close to that of the perfect synchronization in a fixed wireless environment. Here we show that mobility has a negligible effect on the performance of the algorithm. We simulate two methods. Method I utilizes the traditional correlation-based timing synchronizer and picks the maximum correlation point. The second method, the proposed one, utilizes method I for initial coarse synchronization followed by the proposed decision-directed timing adjustment of the previous section. To evaluate the performance of these methods, we measure $P_{error}(m)$, the probability of making a timing error of m sampling periods. Fig. 4 shows the performance in high mobility environments at $\frac{\sigma_X^2 \sigma_H^2}{\sigma_W^2} = 20dB$. The top sub-figure shows the error profile of the correlation-based method in a fixed wireless environment. As the delay spread spans 64% of the guard interval, timing offsets of up to 36% of the guard interval (which becomes 82 sampling points) to the left side can occur without loss of performance. We call this region "*safe zone*", as is marked on Fig. 4. It can be seen that the correlation-based method makes a considerable amount of error out of the safe zone. The middle sub-figure shows the performance of the proposed method in a fixed wireless environment. As can be seen, its error profile is mainly confined to the *safe zone*. To see the impact of mobility, Fig. 4 also shows the performance for different levels of mobility: $f_{d,norm}$ =10%, 20% and 50%. Compared with the no Doppler case, it can be observed that the error profile is not affected by high mobility. This is due to the considerable impact of $factor\#1$ on channel estimation error as was shown in the previous section.

Fig. 5 Channel power–delay profile

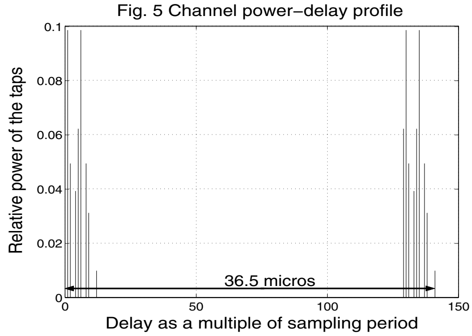

Fig. 4 Performance in high mobility environments

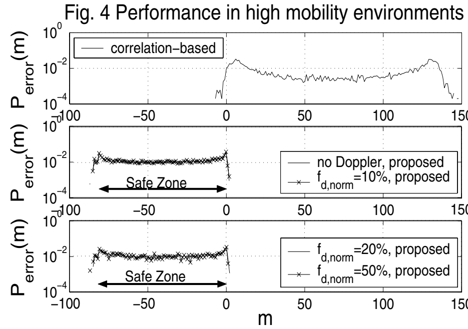

References

[1] Cimini, "Analysis and Simulation of a digital mobile channel using orthogonal frequency division multiplexing," IEEE Trans. Comm., vol. COMM-33, pp. 665-675, July 1985

[2] Y. Mostofi, D. Cox and A. Bahai, "Effect of frame synchronization errors on pilot-aided channel estimation in OFDM: analysis and solution," 5^{th} international symposium on wireless personal multimedia communications, Oct. 2002, pp. 1309-1313

[3] Y. Mostofi, D. Cox and A. Bahai, "ICI Mitigation for Mobile OFDM Receivers," Proceedings of IEEE 38th International Conference on Communications (ICC), May 2003, Anchorage, Alaska

[4] Y. Mostofi, "Timing Synchronization and ICI Mitigation for Pilot-aided OFDM Mobile Systems," PhD Thesis, Stanford University, Nov. 2003

[5] S. Muller, "On the optimality of metrics for coarse frame synchronization in OFDM: a comparison," Ninth IEEE International Symposium on PIMRC, 1998

[6] R. Negi and J. Cioffi, "Pilot tone selection for channel estimation in a mobile OFDM system," IEEE Trans. Consumer Electronics, vol. 44, no. 3, Aug. 98

[7] T. M. Schmidl, "Synchronization algorithms for wireless data transmission using Orthogonal Frequency Division Multiplexing (OFDM)," PhD Dissertation, Stanford university, June 1997

[8] J. Van de Beek, M. Sandell and M. Isaksson, "Low-complex frame synchronization in OFDM systems," Fourth IEEE International Conference on Universal Personal Communications, 1995

[9] B. Yang, K. Letaief and R. Cheng, "Timing recovery for OFDM transmission," JSAC, vol. 18, no. 11, Nov. 2000